The Method of Lines Applied to Planar Transmission Lines in Circular and Elliptical Waveguides

KE WU, MEMBER, IEEE, AND RUEDIGER VAHLDIECK, SENIOR MEMBER, IEEE

Abstract —The method of lines (MOL) is utilized to analyze a class of planar transmission lines with circular or semicircular/elliptical metallic shielding. The paper shows how the general MOL principles can be modified such that curved boundary structures can be included. Dispersion diagrams are presented for microstrip and slotline structures with curved metallic shielding as well as for their suspended counterparts in circular and elliptical waveguides.

I. Introduction

The METHOD of Lines (MOL) is a semianalytical method well suited to the characterization of the dispersive properties and discontinuities of a wide range of transmission lines. The method, originally used for boundary value problems in physics, was further developed by Pregla and coworkers [3]–[6] and other researchers in this field (i.e., [7]–[9]) for application to various forms of waveguiding structures. The advantage of this method in solving the Helmholtz equation for the structure to be analyzed is that it requires cross-sectional discretization in only one direction while the other direction can be treated analytically. There are no specially suited basis functions necessary. The problem of relative convergence is avoided and the MOL can easily be applied to irregularly shaped transmission lines which were previously analyzable only by such methods as the finite element method (FEM) and the transmission line method (TLM).

In previous publications the MOL has been applied to structures on isotropic and anisotropic [7] substrate material covered by rectangular metallic shielding. In the present paper it is shown that the method is equally applicable to transmission line structures with circular or semicircular/elliptical metallic boundaries. This requires a modified formulation of the method which is then applied to an interesting but relatively unstudied form of quasi-planar transmission line: shielded microstrip and slotline as well as their suspended counterparts in circular or elliptical waveguides. Quasi-planar transmission lines of this form are potentially advantageous over structures in rectangular waveguides because generally circular waveguides provide a better control of field polarization, which is useful in particular for phase shifters, traveling-wave isolators, antenna feeds, etc. Furthermore, while increasing attenuation in rectangular waveguides at millimeter-wave frequencies may be prohibitive for certain applications, oversized circular waveguides are a potential alternative. The usefulness of a bilateral finline in a circular waveguide as applied to a wide-bandwidth coupler was described as early as 1955 by Robertson [1]. Since then, however, the possibility of integrating planar transmission lines into circular or elliptical waveguides has been widely neglected. As a consequence, there are almost no data available in the open literature describing the propagation characteristics in this type of hybrid transmission line.

The propagation characteristics of a bilateral finline in a circular waveguide have been studied recently by Costache and Hoefer [2] using a finite element method. But in this approach, large systems of equations must be solved directly, which requires considerable memory space and computing power. Using the MOL, a discrete orthogonal transform is applied and the problem is essentially solved analytically in the transformed domain. This procedure reduces the matrix sizes in the original domain without affecting the accuracy and leads to a significantly faster computer algorithm which is more efficient with regard to memory space and is suitable for personal computers. To verify our theoretical results we have made a comparison with the analytical solution for the circular hollow waveguide as well as with the numerical data for the bilateral finline published in [2]. In both cases the agreement is excellent.

II. Theory

By modifying the method of lines to curved boundaries, we are able to rigorously analyze planar transmission lines in circular and elliptical waveguides. The following will give a brief review of the essential steps in the MOL as far as it is necessary to understand the modifications made.

The cross-sectional view of the type of quasi-planar transmission line to be analyzed in this paper is shown in Fig. 1. Any attempt to calculate the propagation characteristics with the mode matching technique or the spectral-domain method would lead to Bessel functions in case of the circular shield or to Mathieu functions in case of the

Manuscript received March 23, 1989; revised July 14, 1989. This work was supported in part by the National Science and Engineering Research Council of Canada.

The authors are with the Department of Electrical and Computer Engineering, University of Victoria, P.O. Box 1700, Victoria, B.C., Canada V8W 2Y2.

IEEE Log Number 8930944.

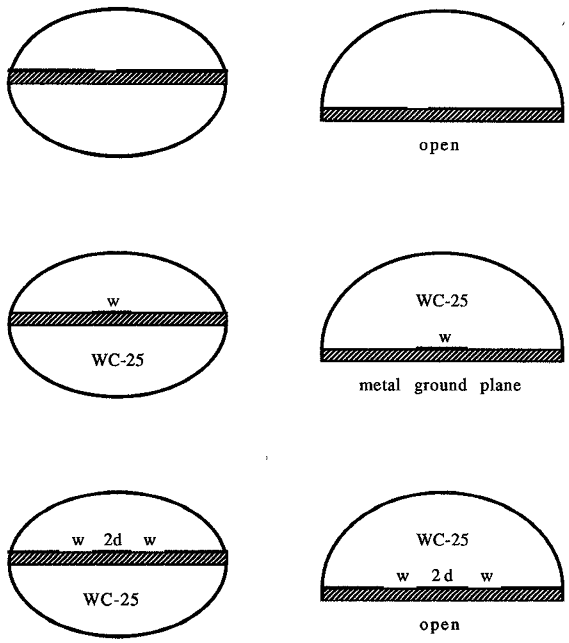

Fig. 1. Quasi-planar transmission lines in circular/elliptical, closed, and semiopen waveguides.

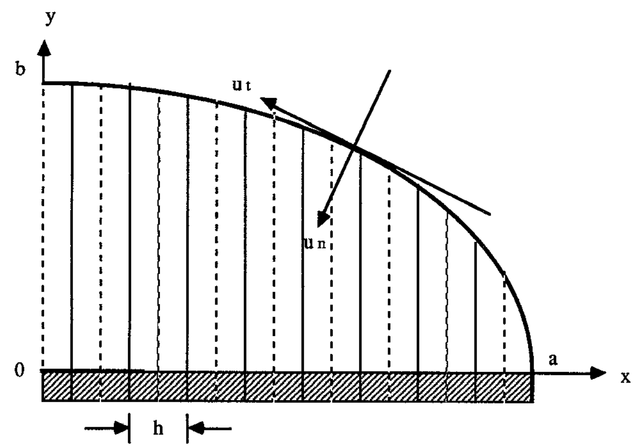

Fig. 2. Cross section of the semiopen stripline in an elliptical enclosure. For the following structures, $\epsilon_r = 2.22$ and substrate thickness = 254 μm.

elliptical shield. In both cases it is difficult or impossible to match the respective eigenfunctions at the interface to the planar circuit. In the method of lines this problem can be avoided by discretizing the entire cross section in one direction such that the discretization lines are perpendicular to the planar circuit regardless of the location of the housing walls. In a rectangular waveguide the lines are either perpendicular or tangential to the metallic enclosure. In a circular housing there are only two locations at which this is the case. Between the two locations the boundary conditions must follow the curvature of the housing described by the function

$$\frac{x^2}{a^2}+\frac{y^2}{b^2}=1 \tag{1}$$

where a and b are the semiaxis lengths in the x and y directions in Fig. 2. To explain the principal steps in the MOL the symmetrical semicircular/elliptical stripline is chosen as shown in Fig. 2. An extension of the method to more complicated structures is straightforward. The electromagnetic field in each homogenous subregion is described by two scalar potential functions Ψ^e and Ψ^h which both satisfy the Helmholtz equation. Initially the assumption is also made that the boundary conditions are satisfied along the curved metallic enclosure at the symmetry walls. It will be shown later under which conditions this is true. All field components are found from

$$\vec{E}=\frac{1}{j\omega\epsilon}\nabla\times\nabla\times(\Psi^e\vec{ez})-\nabla\times(\Psi^h\vec{ez})$$

$$\vec{H}=\nabla\times(\Psi^e\vec{ez})+\frac{1}{j\omega\mu}\nabla\times\nabla\times(\Psi^h\vec{ez}). \tag{2}$$

To solve this hybrid field problem numerically, the cross section is discretized in the x direction with an equi-mesh-width h. The discretization lines of Ψ^h are shifted by $h/2$ with respect to the lines of Ψ^e. Thus, the lateral boundary conditions can easily be fitted and the discretization errors are reduced significantly. For symmetrical structures the first discretization line for the electric or magnetic potential starts at the electric or magnetic wall, respectively (Fig. 2), which corresponds to a Dirichlet–Dirichlet (D–D) or Neumann–Dirichlet (N–D) boundary condition. The mesh size h can be obtained by taking two conditions into account simultaneously: a) the lateral boundary conditions at $x=0,\ y=[0,b]$ and $x=a,\ y=0$ (Fig. 2) and b) the edge conditions at $x=w/2,\ y=0$.

From the edge condition we obtain

$$h=\frac{W}{2(N_0^e+0.25)-0.5\delta_{em}} \tag{3}$$

$$\delta_{em}=\begin{cases}0 & \text{electric wall}\\ 1 & \text{magnetic wall}\end{cases} \tag{4}$$

$$N_{\text{total}}^e=N_0^e+\text{int}\left[\frac{\left(a-\frac{W}{2}\right)}{h}-0.75\right] \tag{5}$$

where N_0^e is the total number of e lines on the strip and N_{total}^e is the total number of e lines over the cross section. By choosing the number of lines on the strip the total number of e lines over the cross section is automatically determined. All potential functions at the discrete points can be arranged in an ordered vector form. It should be noted that the resulting vectors and matrices with the superscript e or h are of order N^e or N^h, respectively. The finite difference expression of the first and second derivatives of Ψ^h and Ψ^e can then be written in matrix form:

$$\frac{\partial\Psi^e}{\partial_x}\to\frac{[D_x]}{h}[\Psi^e] \tag{6}$$

$$\frac{\partial\Psi^h}{\partial_x}\to-\frac{[D_x]^t}{h}[\Psi^h] \tag{7}$$

$$\frac{\partial^2\Psi^e}{\partial_x^2}\to-\frac{[D_x]^t[D_x]}{h^2}[\Psi^e] \tag{8}$$

$$\frac{\partial^2\Psi^h}{\partial_x^2}\to-\frac{[D_x][D_x]^t}{h^2}[\Psi^h]. \tag{9}$$

Now the x-dependent variables are discretized and are available in vector form. They automatically include the lateral boundary and edge conditions.

Substituting the matrix expressions (8), (9) into the Helmholtz equations, one-dimensional differential matrix equations are obtained in the discrete domain in which all elements are coupled to each other:

$$\frac{d^2[\Psi^e]}{d_y^2} - \left[\frac{[D_x]^t[D_x]}{h^2} + \beta^2 - k^2\right][\Psi^e] = 0 \quad (10)$$

$$\frac{d^2[\Psi^h]}{d_y^2} - \left[\frac{[D_x][D_x]^t}{h^2} + \beta^2 - k^2\right][\Psi^h] = 0. \quad (11)$$

The second-order operators $[D_x]^t[D_x]$ and $[D_x][D_x]^t$ are real, symmetric, and tridiagonal matrices. Thus, they can be transformed by a simple orthogonal transformation into diagonal form with real positive and distinct eigenvalues:

$$[T^e]^t[D_x]^t[D_x][T^e] = [\lambda^e] \quad (12)$$

$$[T^h]^t[D_x][D_x]^t[T^h] = [\lambda^h]. \quad (13)$$

$[T^e]$ and $[T^h]$ are the matrices of eigenvectors which are available in analytical form for equidistant discretization [5]. It can be proved that the bidiagonal first-order operator $[D_x]$ is transferred into quasi-diagonal or quasi-subdiagonal form by the following transformation:

$$[T^h]^t[D_x][T^e] = [\delta] \quad (14)$$

$$[T^e]^t[D_x]^t[T^h] = [\delta]^t. \quad (15)$$

Based upon (12) and (13), the following relationship holds:

$$[\lambda^e] = [\delta]^t[\delta] \quad (16)$$

$$[\lambda^h] = [\delta][\delta]^t. \quad (17)$$

With the above decoupling procedure the partial differential equations can now be written as a system of ordinary differential equations:

$$\frac{d^2[\phi^{e,h}]}{d_y^2} - [k^{e,h}][\phi^{e,h}] = [0] \quad (18)$$

$$[\gamma^{e,h}] = [\lambda^{e,h}]\frac{1}{h^2} + (\beta^2 - k^2)[I] \quad (19)$$

with $[I]$ being the identity matrix and $[\phi^{e,h}] = [T^{e,h}][\Psi^{e,h}]$. The general solution of (18) can be written as a set of inhomogeneous transmission line wave equations in discrete form, assuming that the lines $\Psi^{e,h}$ pass through a homogeneous dielectric layer from $y = y_1$ to $y = y_2$:

$$\begin{pmatrix} [\phi] \\ \left[\frac{d\phi}{dy}\right] \end{pmatrix}_{y_2} = \begin{pmatrix} \cosh\gamma^{e,h}(y_2 - y_1) & \frac{1}{\gamma^{e,h}}\sinh\gamma^{e,h}(y_2 - y_1) \\ \gamma^{e,h}\sinh\gamma^{e,h}(y_2 - y_1) & \cosh\gamma^{e,h}(y_2 - y_1) \end{pmatrix} \cdot \begin{pmatrix} [\phi] \\ \left[\frac{d\phi}{dy}\right] \end{pmatrix}_{y_1}. \quad (20)$$

The matrix equation (20) is a function of y at discrete points in the x direction. The boundary conditions, once they are satisfied at one location, are assumed to be satisfied automatically at each x coordinate along the boundary. However, this is only true in a rectangular waveguide housing. For a curved waveguide housing, the field components tangential (E_t) and normal (H_n) to the boundary are composed of vector components which vary depending on the x location. For example, at $x = 0$ and $y = b$ (Fig. 2), the E_x and H_y components become zero by setting ϕ^e and $d\phi^h/d_y$ equal to zero. Moving along the boundary, both vectors increase to a maximum value at $x = a$ and $y = 0$ (Fig. 2). This variation in the boundary conditions must be incorporated into the discretization procedure. This can be done by rewriting (1) in terms of the tangential and normal unity vectors (see Fig. 2) in the following way:

$$\vec{U}_t = \frac{\vec{x} + \frac{d_y}{d_x}\vec{y}}{\sqrt{1 + \left(\frac{d_y}{d_x}\right)^2}} \quad (21)$$

$$\vec{U}_n = \frac{-\vec{x} + \left(\frac{d_x}{d_y}\right)\vec{y}}{\sqrt{1 + \left(\frac{d_x}{d_y}\right)^2}}. \quad (22)$$

If we now apply the boundary conditions of zero tangential electric field and zero normal magnetic field in the original domain, we obtain two matrix equations with inner products at each discrete point

$$|\vec{U}_t| \cdot \left[\vec{E}_x + \vec{E}_y\right] = 0 \quad (23)$$

$$|\vec{U}_n| \cdot \left[\vec{H}_x + \vec{H}_y\right] = 0 \quad (24)$$

$$\left[\vec{E}_z\right] = 0. \quad (25)$$

Even though the Ψ^e lines are shifted with respect to the Ψ^h lines in the space domain, the derivative of the housing function d_y/d_x holds at every Ψ^e and Ψ^h line. The field components in (23)–(25) are derived from (2) and the following relationship can be obtained in the original domain:

$$[\Psi^e] = 0 \quad (26)$$

$$\left[\frac{d\Psi^h}{d_y}\right] = \left[\frac{d_y}{d_x}\right] \cdot \left[\frac{d\Psi^h}{d_x}\right]. \quad (27)$$

Transforming (26) and (27) into the transform domain yields

$$[\phi^e] = 0 \quad (28)$$

$$\left[\frac{d\phi^h}{d_y}\right] = [T^h]^t\left[\frac{d_y}{d_x}\right][D^h][T^h][\phi^h]. \quad (29)$$

Note that the derivative matrix $[d_y/d_x]$ is equally related to e as well as to h lines because of the full spatial inner product and regardless of the e- and h-line shift in the discrete domain.

It follows from (28) and (29) that $[\phi^e]$ remains always zero for all kinds of curved boundaries since $[\phi^e]$ is associated with the E_z field component. The quantity $[d\phi^h/d_y]$ becomes zero if $d_y/d_x = 0$. It should be noted that the vector form of $[d\phi^h/d_y]$ depends on the lateral boundary conditions (at $x = 0$, $y = [0, b]$ and $x = a$, $y = 0$) and can also implicitly be found in $[T^{e,h}]$ and $[\delta^t]$. The latter means that elements of the vector $[d\phi^h/d_y]$ may be coupled to each other. In the limiting case (noncurved or piecewise-straight waveguide), $[d\phi^h/d_y]$ equals zero.

It is worth mentioning that there are two singular points at $x = \pm a$ where d_y/d_x becomes infinity. This results from the fact that $d\phi^h/d_y$ at both sides tends to approach infinity, which requires some precautions in the numerical procedure.

From the transmission line equation (20), considering the boundary conditions along the curved enclosure as well as the continuity condition at the interface at $y = 0$, an inhomogeneous matrix equation is obtained:

$$\begin{pmatrix} [\tilde{E}_x] \\ [\tilde{E}_z] \end{pmatrix} = \begin{pmatrix} [\tilde{Z}_{xx}] & [\tilde{Z}_{xz}] \\ [\tilde{Z}_{zx}] & [\tilde{Z}_{zz}] \end{pmatrix} \begin{pmatrix} [\tilde{J}_x] \\ [\tilde{J}_z] \end{pmatrix}. \tag{30}$$

The submatrices $[\tilde{Z}_{xx}]$ and $[\tilde{Z}_{zz}]$ are diagonal, and $[\tilde{Z}_{xz}]$ and $[\tilde{Z}_{zx}]$ are diagonal or subdiagonal, depending on the lateral conditions in the transformed domain.

After transformation back into the original domain [5], a considerably reduced matrix equation is obtained by setting the tangential field components at the metallic strip to zero:

$$[Z(\beta)] \begin{pmatrix} [J_x] \\ [J_z] \end{pmatrix} = 0. \tag{31}$$

From here the propagation constants are found for all zeros of $\det\{Z(\beta)\}$.

In general, the number of lines necessary to accurately analyze a given cross section depends on the finest details to be resolved in the structure. Therefore, in the following analysis the number of lines is determined by the strip/slot dimensions. It was found that for a strip-type transmission line a minimum of two Ψ^h lines and one Ψ^e line across the strip width was necessary and vice versa for slot-type transmission lines.

III. Numerical Results

In order to examine the reliability and performance of this modified approach, we have analyzed microstrip and slotline structures in circular/elliptical waveguide housings. We have first analyzed the standard circular waveguide (WC-25, radius = 3.175 mm, $f_c(\mathrm{TE}_{11}) = 27.686$ GHz) and compared the numerical data with analytical results. It was found that there is perfect agreement between the numerical and the analytical solution of the fundamental mode dispersion characteristic over the frequency range of interest.

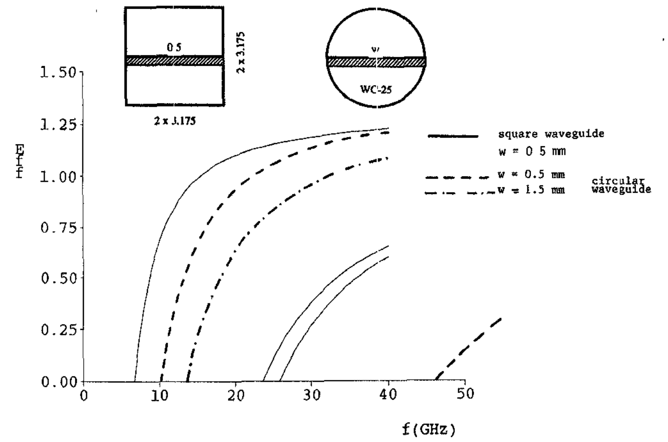

Fig. 3. Unilateral finline in square and circular waveguide. WC-25 = 3.175 mm × 3.175 mm.

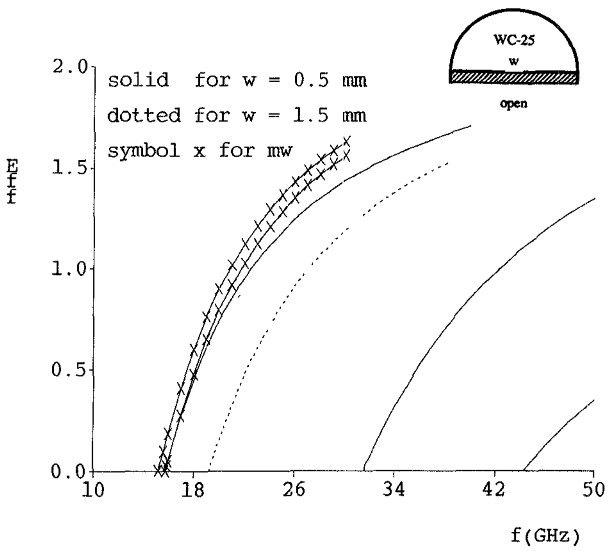

Fig. 4. Dispersion of a slotline in a circular semiopen enclosure.

Then a comparison was made between a unilateral finline in a square waveguide and a circular waveguide. It is clear from Fig. 3 that the monomode range in a circular housing greatly exceeds that in the square waveguide. Even the monomode range in a rectangular waveguide is less than in the circular case since the second higher order mode starts to propagate at 42 GHz (*Ka*-band) whereas in the circular guide the second mode cutoff frequency is at 47 GHz. For the circular waveguide the modes shown in Fig. 3 are obtained from electric wall symmetry. The HE1 mode can thus be traced back to the TE_{11} mode in the empty waveguide. As expected, the HE1 mode is mainly confined within the slot region of the guide and therefore is strongly influenced by the slot width. For magnetic wall symmetry no further modes were found up to 50 GHz. This is in contrast to the results in a semicircular waveguide enclosure when the ground plane is removed (semiopen). For this case Fig.4 shows three fundamental modes close together having a cutoff frequency around 15 GHz. Two of the modes show magnetic wall symmetry and one

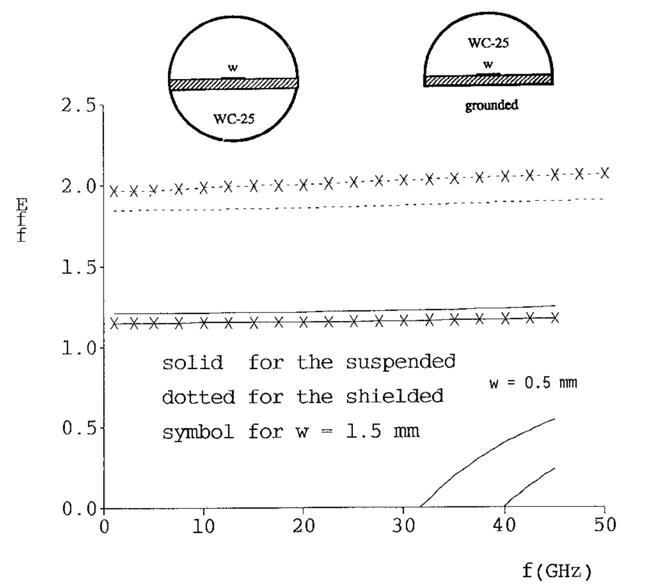

Fig. 5. Propagation characteristics in suspended and grounded stripline.

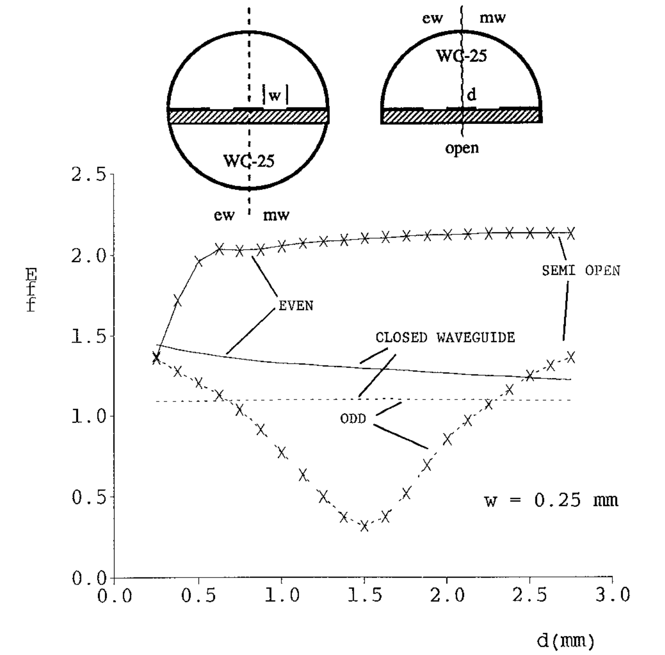

Fig. 6. Propagation constant in coplanar transmission lines shielded by closed and semiopen waveguides.

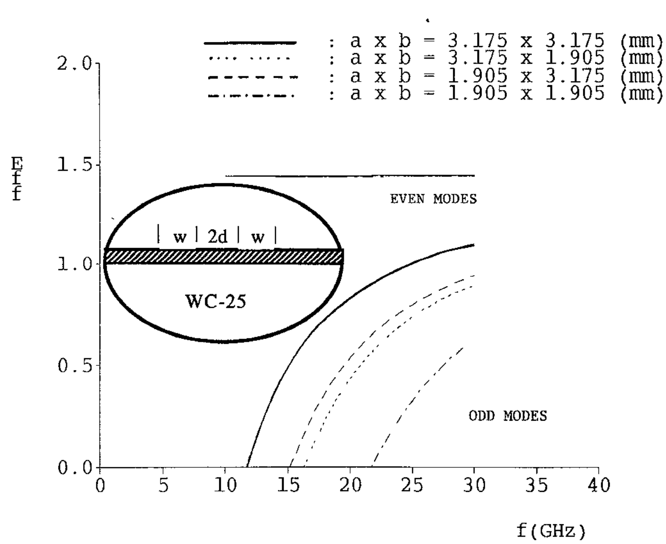

Fig. 7. Effect of circular and elliptical waveguide shapes on mode propagation in a coplanar transmission line.

electric wall symmetry. The modes with magnetic wall symmetry are virtually insensitive to variations in the slot width whereby the third mode (electric wall symmetry) cutoff frequency is reduced when the slot width decreases. This indicates that this mode originates from the TE_{11} mode of the empty circular guide. For comparison, the unilateral finline in a square waveguide with semiopen boundary shows also three fundamental modes with the same magnetic wall and electric wall symmetry [10]. Fig. 5 shows the suspended microstrip in a circular metallic enclosure (WC25) and its grounded counterpart in a semicircular metallic enclosure. As expected, the quasi-TEM mode of the grounded structure is much higher, increasing further for wider strip width. This is in contrast to the suspended microstrip line, where the propagation constant decreases for wider strip width. It should also be noted that the higher order modes in the suspended case start to propagate at much higher frequencies than for the same transmission line in a rectangular waveguide. For instance, in a *Ka*-band housing the first waveguide mode starts to propagate around 20 GHz (for the planar structure suspended in the *E* plane as well as the *H* plane) and in the circular housing around 32 GHz. Fig. 6 shows even and odd modes of a coplanar transmission line in a circular and semicircular waveguide versus the slot width d. It is interesting to note that for the semicircular case and the ground plane removed the odd mode shows a minimum ϵ_{eff} at $d = 1.5$ mm. A comparative analysis for circular and elliptical waveguide enclosures is shown in Fig. 7 for a coplanar transmission line. It is obvious that the quasi-TEM mode, the even mode, remains relatively undisturbed by changing from one focal point into two (elliptical waveguide), regardless of whether this change occurs in the y or the x direction. The cutoff frequencies of higher order modes, however, move up towards higher frequencies in the elliptical waveguide. The interesting point is that by changing b from 3.175 mm to $b = 1.905$ mm the occurrence of the first waveguide mode can be shifted 5 GHz towards higher frequencies. Fig. 8 shows that there is no noticeable effect on the quasi-TEM mode at higher frequencies in a suspended stripline. Only at lower frequencies does the difference between circular and elliptical housings become visible.

IV. Conclusion

This paper introduced a modified approach to the method of lines to allow the treatment of curved boundary value problems. For the first time the MOL has been applied to the analysis of a variety of quasi-planar transmission lines in circular/elliptical and semicircular waveguides with partially open boundaries. Results have shown

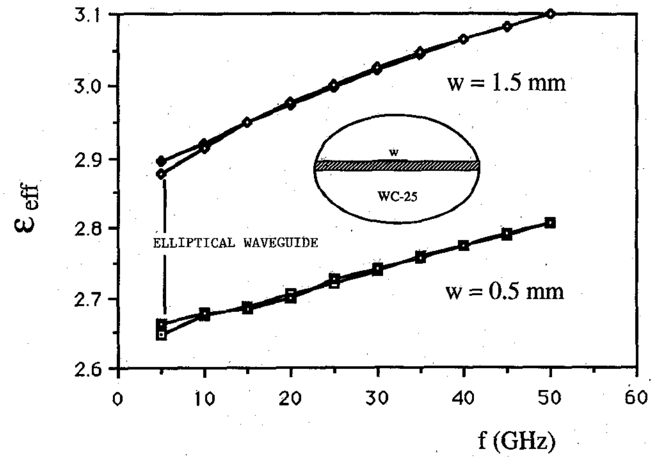

Fig. 8. Dispersion of the quasi-TEM mode in a circular ($a = b =$ 3.175 mm) and an elliptical ($a = 4.17$ mm, $b = 3.175$ mm) waveguide.

that some of the structures have potential applications at millimeter-wave frequencies because losses in circular waveguide enclosures are generally lower than in rectangular waveguides. A more detailed study including losses of different modes, as well as the characteristic impedance, is currently in progress. Our experience so far has shown that the method of lines is numerically more efficient than other methods applicable to the same problem and that, as evidenced by this paper, odd shaped boundary value problems can be handled quite easily.

References

[1] S. D. Robertson, "The ultra-bandwidth finline coupler," *Proc. IRE*, vol. 43, pp. 739–741, June 1985.

[2] Eswarappa, G. Costache, and W. J. R. Hoefer, "Finlines in rectangular and circular waveguide housings including substrate mounting and bending effects—Finite element analysis," *IEEE Trans. Microwave Theory Tech.*, vol. 37, pp. 299–306, Feb. 1989.

[3] U. Schulz and R. Pregla, "A new technique for the analysis of the dispersion characteristics of planar waveguides," *Arch. Elek. Übertragung*, vol. 34, pp. 169–173, 1980.

[4] U. Schulz, "On the edge condition with the method of lines in planar waveguides," *Arch. Elek. Übertragung*, vol. 34, pp. 176–178, 1980.

[5] S. Worm and R. Pregla, "Hybrid-mode analysis of arbitrarily shaped planar microwave structures by the method of lines," *IEEE Trans. Microwave Theory Tech.*, vol. MTT-32, pp. 191–196, Feb. 1986.

[6] H. Diestel, "A quasi-TEM analysis for curved and straight planar multiconductor systems," *IEEE Trans. Microwave Theory Tech.*, vol. 37, pp. 748–753, Apr. 1989.

[7] B. M. Sherrill and N. G. Alexopoulos, "The method of lines applied to a finline/strip configuration on an anisotropic substrate," *IEEE Trans. Microwave Theory Tech.*, vol. MTT-35, no. 6, June 1987.

[8] Z. Chen and B. Gao, "Deterministic approach to full-wave analysis of discontinuities in MIC's using the method of lines," *IEEE Trans. Microwave Theory Tech.*, vol. 37, pp. 606–611, Mar. 1989.

[9] A. G. Keen, M. J. Wale, M. I. Sobhy, and A. J. Holden, "Analysis of electro-optic modulators by the method of lines," in *Proc. 17th European Microwave Conf.* (Rome), Sept. 1987, pp. 917–922.

[10] K. Wu and R. Vahldieck, "On the analysis of quasi-planar transmission lines in circular/elliptical waveguides using the method of lines," in *IEEE MTT-S 1989 Int. Microwave Symp. Dig.* (Long Beach, CA), pp. 503–506.

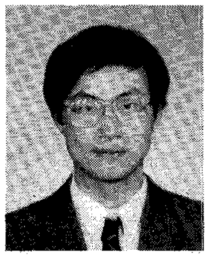

Ke Wu (M'87) was born in Jiangsu, China, on December 9, 1962. He received the B.Sc. degree (with distinction) in radio engineering from the Nanjing Institute of Technology, Nanjing, China, in 1982 and the D.E.A. degree in electronics and the Ph.D. degree (with distinction) in optics, optoelectronics, and microwave engineering from the Institut National Polytechnique de Grenoble (INPG), Grenoble, France, in 1984 and 1987, respectively.

During the years 1983–1987, he conducted research in the Laboratoire d'Eléctromagnetisme, Microondes et Optiques guidés (LEMO), Grenoble, France. Since 1988 he has been a postdoctoral research associate in the Department of Electrical and Computer Engineering at the University of Victoria, Victoria, B.C., Canada. His main research interests include electromagnetic fields, numerical methods, analysis and design of various microwave/millimeter-wave integrated and monolithic circuits, electro-optic and optoelectronic components, planar antennas, and microwave/optical signal processing.

Dr. Wu received a Chinese Overseas Graduate Fellowship in 1982, a U.R.S.I. Young Scientist Award in 1987, and, together with two coauthors, the Oliver Lodge Premium from the IEE for the outstanding publication in 1988.

Ruediger Vahldieck (M'85–SM'86) received the Dipl.-Ing. and Dr.-Ing. degrees in electrical engineering from the University of Bremen, Bremen, West Germany, in 1980 and 1983, respectively.

From May 1984 to June 1986 he was a Research Associate at the University of Ottawa, Ottawa, Canada, and in July 1986 he joined the Electrical and Computer Engineering Department of the University of Victoria, Victoria, Canada, where he is now an Associate Professor. His research interests include numerical methods to solve electromagnetic field problems for computer-aided design of microwave and millimeter-wave integrated circuits, FET amplifiers, couplers, and nonreciprocal devices. The emphasis of his work is on quasi-planar filters and filters for MMIC application.

Dr. Vahldieck, together with three coauthors, received the outstanding publication award of the Institution of Electronic and Radio Engineers in 1983. He is on the editorial board of the IEEE Transactions on Microwave Theory and Techniques and has published 40 technical papers in the field of microwave CAD. He teaches professional short courses at George Washington University, Washington, DC, on numerical techniques in electromagnetics. He is the owner of EHF Technologies, a software, MIC design, and consulting company.